Water Soluble Polymers. 75. Responsive Microdomains in Labeled *N*-Octylamide-Substituted Poly(sodium maleate-*alt*-ethyl vinyl ether): Transient Fluorescence and Time-Resolved Fluorescence Anisotropy Studies

Yuxin Hu, R. Scott Armentrout, and Charles L. McCormick*

Department of Polymer Science, University of Southern Mississippi, Southern Station Box 10076, Hattiesburg, Mississippi 39406

Received December 2, 1996; Revised Manuscript Received April 10, 1997[⊗]

ABSTRACT: Dansyl fluorescent labels with two different spacer lengths (D2 and D8) were pendently attached to unmodified and 30 mol % *n*-octyl-modified copoly(sodium maleate-*alt*-ethyl vinyl ether). The time-resolved fluorescence anisotropy (TRFA) measurements of these labels were obtained in aqueous media as a function of pH and analyzed using impulse reconvolution analysis (IRA). At pH values below 6.7, the hydrophobically modified copolymers exist as compact globules, as evidenced by the long fluorescence emission lifetimes of the labels. At these pH values, two rotational correlation times (RCTs) corresponding to two distinct molecular motions within associating hydrophobic microdomains are seen: one associated with the motion of the chromophore coupled to the copolymer backbone and the other associated with the rotational motion of the chromophore. Above pH 6.7, the copolymer is progressively extended with increasing pH, as indicated by the short emission lifetime of the labels and the observation of only one rotational correlation time corresponding to the rotational motion of the labels in an aqueous environment. Local rotational diffusion coefficients and local viscosities for the dansyl labels have also been estimated as a function of pH. The observed fluorescence data are consistent with the classic model proposed for pH-induced transition from a polysoap to an extended polyelectrolyte in dilute aqueous solution.

Introduction

Time-resolved fluorescence anisotropy (TRFA) has been widely used for studying segmental mobility and conformational changes in polyelectrolytes[1−3] and proteins.[4,5] Synthetic polymers that have been studied include polyacrylamide,[6,7] poly(*N*-isopropylacrylamide),[8] polystyrene−poly(methyl methacrylate) graft copolymers,[9] and polystyrene-*block*-poly(methacrylic acid).[10] The dansyl chromophore is often chosen as a fluorescent label for assessing the microstructural organization of polymers in solution due to its environmentally sensitive emission quantum yield, fluorescence emission wavelength, and lifetime.[11−14] One of its strongest attributes, however, is that its fluorescence anisotropy properties are extremely sensitive to changes in the surrounding microenvironment.[1,8,15] Binkert and Ricka et al.,[6,8] for example, measured the segmental mobility of the dansyl label attached to poly(*N*-isopropylacrylamide) by measuring the TRFA as a function of changes in temperature. A restricted rotational rigid ellipsoid model was used to calculate an effective diameter of the dansyl label environment and the dynamic persistence length of the polymer backbone. Subsequently, Horie et al.[15] found that steady-state fluorescence anisotropy (SSFA) measurements using dansyl labels differed from similar TRFA measurements in polyacrylamide hydrogels. The authors suggested that SSFA, for the most part, gauges the free rotational motion of the dansyl labels, whereas TRFA measures the rotational and translational motion of the labels.

In the previous paper of this series,[16] unmodified and 30% *n*-octylamide hydrophobically modified copoly(sodium maleate-*alt*-ethyl vinyl ether) [copoly(SM−EVEs)] were prepared by incorporating dansyl fluorescent labels having different spacer lengths. These domain-forming copolymers belong to a class of polymers that exhibit the well-characterized polysoap-to-polyelectrolyte transition, as was first illustrated by Strauss.[17] Photophysical techniques were used to characterize polymer conformational changes and association behavior in response to changes in pH and ionic strength. Intra- and interpolymer associations were probed by monitoring steady-state fluorescence and nonradiative energy transfer of fluorescent labels covalently bound to the modified copolymer backbone.

In this paper, further photophysical studies are reported that examine the dynamic processes governing the association of hydrophobically modified water-soluble polymers. We performed both SSFA and TRFA studies as a function of pH for the dansyl labels covalently bound to unmodified and 30% octylamide-modified copoly(SM−EVEs) by spacers of two different lengths. Results from the impulse reconvolution analysis (IRA) of the TRFA were compared with those from the SSFA. In addition, the rotational diffusion coefficients were examined for both long- and short-spaced dansyl labels. Such studies yield valuable information about local viscosity and mobility in associative microheterogeneous domains. Utilizing these techniques, we compare the local viscosity within microheterogeneous domains to that near the polymer backbone in aqueous media.

Experimental Section

Materials and Sample Preparation. The *n*-octylamide-modified copoly(SM−EVEs) with D2 and D8 dansyl labels (Chart 1) were synthesized, and all aqueous polymer solutions were prepared as described in the previous paper of this series.[16] In Chart 1, C0, C8, D2, and D8 represent unmodified, 30 mol % *n*-octyl-modified, short- and long-spaced dansyl labels, respectively. The M_w of the copoly(maleic anhydride-*alt*-ethyl vinyl ether) is 2.2×10^5 in THF solution and the M_w of the 30 mol % *n*-octyl hydrophobically modified copoly(SM−

[⊗] Abstract published in *Advance ACS Abstracts,* May 15, 1997.

S0024-9297(96)01753-6 CCC: $14.00

Chart 1. Structures of Hydrophobically Modified Copoly(sodium maleate-*alt*-ethyl vinyl ethers) with Fluorescent Labels

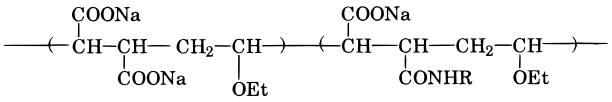

R = n-Octyl (C8), D2, D8

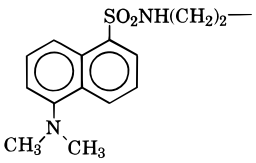

D2

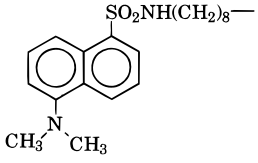

D8

Table 1. Description of Solution Compositions[a]

Short-Spaced Labels with C8-Modifiied Copoly(SM−EVEs)			
solution	[C8] (g/L)	[C8-D2] (g/L)	[dansyl] (μmol/L)
C8/C8-D2	0.25	0.25	9.6
Long-Spaced Labels with C8-Modified Copoly(SM−EVEs)			
solution	[C8] (g/L)	[C8-D8] (g/L)	[dansyl] (μmol/L)
C8/C8-D8	0.25	0.25	9.5
Short-Spaced Labels Copoly(SM−EVEs)			
solution	[C0] (g/L)	[C0-D2] (g/L)	[dansyl] (μmol/L)
C0/C0-D2	0.25	0.25	10.7
Long-Spaced Labels Copoly(SM−EVEs)			
solution	[C0] (g/L)	[C0-D8] (g/L)	[dansyl] (μmol/L)
C0/C0-D8	0.25	0.25	10.6

[a] C8: 30% octyl-modified (SM−EVE). C8-D2: 30% octyl-modified (SM−EVE) with short-dansyl spacer (D2). C8-D8: 30% octyl-modified (SM−EVE) with long-dansyl spacer (D8). C0: unmodified (SM−EVE). C0-D2: unmodified (SM−EVE) with short-dansyl spacer (D2). C0-D8: unmodified (SM−EVE) with long-dansyl spacer (D8).

EVEs) is 3.5×10^5 in aqueous solution as determined by classical light scattering. The compositions for each of the copolymer solutions used in this paper are shown in Table 1.

Instrumentation and Measurements. UV−vis spectra were recorded with a Hewlett-Packard 8452A diode array spectrophotometer, and the fluorescence spectra were measured at 25 °C with an Edinburgh T-Geometry fluorometer. For all fluorescence decay and TRFA measurements, a hydrogen flash lamp was used at 0.40 bar, with slit widths set at 10.0 nm for both the excitation and emission positions. The instrumental response function (IRF) was obtained at 330 nm using a dilute colloidal suspension of dried nondairy creamer. Through analysis of the IRF it was determined that the flash lamp remained stable for a period of ~60 h. The time-resolved fluorescence spectra and anisotropy decays of the dansyl labels were measured at 540 nm using a 330 nm excitation for up to 50 h. The emission intensities transmitted by a polarizer and analyzed in planes parallel, $I_{VV}(t)$, and perpendicular, $I_{VH}(t)$, to the planes of the vertically polarized excitation light were collected for TRFA measurements of the dansyl-labeled polymers. In the measurements of TRFA and SSFA, an instrumental geometry correction factor, $G(\lambda) = I_{HH}(t)/I_{HV}(t)$, was determined for each sample from the ratio of the horizontally polarized emission intensity to the vertically polarized emission intensity using horizontally polarized excitation. The instrumental geometry correction factor, $G(\lambda)$, is used to compensate for the depolarization characteristics of the instrument, which has grating-type monochromators. The G value was measured for every sample. The sum decay from TRFA, $S(t) = I_{VV}(t) + G(\lambda)I_{VH}(t)$, as the fluorescence emission at 540 nm with an excitation wavelength of 330 nm was utilized in order to avoid the effect of depolarization of the chromophore at the moment of excitation. The IRF was used for fitting the fluorescence emission decay curves and the difference decay components from TRFA.

All data were analyzed using a Level 2 GEM software package from Edinburgh Instruments Ltd. The best fit of the fluorescence emission and the TRFA curves was analyzed using a number of statistical methods: reduced χ^2, symmetry of residuals, serial correlation coefficients, and autocorrelation of residuals. The details of these statistical methods may be obtained elsewhere.[18]

Analysis Methods. Since fluorescence emission decay measurements are statistical in nature and the fluorescent labels are randomly attached to the copolymer backbone, fluorescence lifetime distribution analysis (FLDA) (determined by a maximum entropy algorithm) was utilized for fitting the fluorescence emission decays of the dansyl labels. The fluorescence lifetime was obtained from the mean of the lifetime distribution. The fitting function of the fluorescence lifetime is

$$I(t) = \sum A_i \exp(-t/\tau_i) \tag{1}$$

where $i = 1$ or 2 depending on the fluorescence emission decay curve, τ_i is the fluorescence lifetime, and A_i is the pre-exponential factor.

The Perrin−Weber equation[19] (eq 2) was used to calculate the overall rotational correlation time, θ, and rotational diffusion coefficient, D, of the dansyl labels from the SSFA measurements.

$$r_0/\langle r\rangle = 1 + \tau/\theta = 1 + 6D\tau \tag{2}$$

$\langle r\rangle$ is the average steady-state anisotropy in the emission region of the peak wavelength (±35 nm) and is independent of the emission wavelength in these measurements, τ is the emission lifetime, and r_0 represents the limiting value of $\langle r\rangle$ in a medium where no rotational diffusion occurs and Brownian motion is frozen. r_0 has been determined experimentally to be 0.325 for the dansyl chromorphore.[11]

The TRFA decay measurements involve analyzing the orthogonal components of intensity in the planes parallel, $I_{VV}(t)$, and perpendicular, $I_{VH}(t)$, to the planes of the vertically polarized excitation light. The observed TRFA decay, $r(t)$, is then given by

$$r(t) = \frac{I_{VV}(t) - GI_{VH}(t)}{I_{VV}(t) + 2GI_{VH}(t)} = \frac{D(t)}{S(t)} \tag{3}$$

where G is the instrumental geometry correction factor [$G = I_{HH}(t)/I_{HV}(t)$], $S(t)$ is the sum decay from TRFA [$S(t) = I_{VV}(t) + GI_{VH}(t)$], and $D(t)$ corresponds to the difference decay components [$D(t) = I_{VV}(t) - GI_{VH}(t)$].

Impulse reconvolution analysis was used for the TRFA analysis.[2,20,21] TRFA, $r(t)$, was obtained by using the best fit impulse response function, $S(t)$, and the reconvolution fit of the difference decay, $D(t)$, by eq 4.

$$D(t) = r(t)\cdot S(t) \tag{4}$$

Results and Discussion

In our previous paper,[16] we followed the pH-induced globule-to-extended chain conformational change in 30 mol % *n*-octyl-modified copoly(SM−EVEs) utilizing steady-state fluorescence and nonradiative energy transfer (NRET) techniques along with dynamic light scattering, viscometry, and quenching studies. These copolymers undergo a classical polysoap-to-polyelectrolyte (globule-to-extended chain) conformational change with increasing pH. An important aspect of that report was a dramatic decrease in NRET for *n*-octylamide (C8)-modified copoly(SM−EVEs) with transition from a

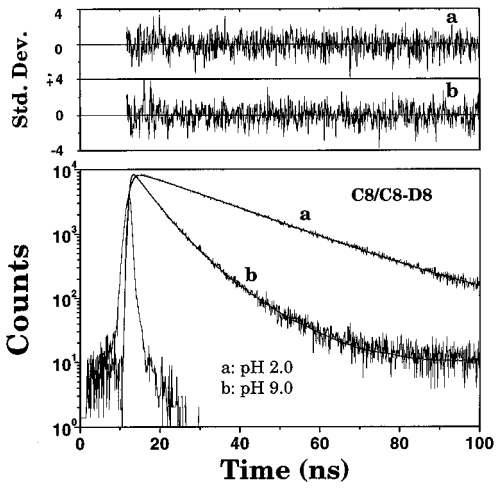

Figure 1. Typical fluorescence decays, fitting curves, and their standard residuals calculated by using lifetime distribution analysis for C8-modified polymers with long-spaced dansyl labels (C8/C8-D8) at a pH value of 2.0 (a) and 9.0 (b). λ_{ex} = 330 nm and λ_{em} = 540 nm.

constricted conformation at low pH to an open, extended form at high pH in dilute solution. Multichain aggregation was shown to be present at low pH in dilute solution and above a pH dependent, critical concentration (C^*) in semidilute aqueous solution. Both long- and short-spacer lengths between the components of the energy transfer pair and the polymer backbone were investigated. Long spacers allowed the respective dansyl and naphthyl moieties to partition into hydrophobic microdomains more easily than the short spacers.

An objective of the present study is to utilize transient fluorescence and TRFA measurements to study label motion and partitioning into hydrophobic microdomains as a function of pH. Structures of the copolymers with dansyl labels tethered by long and short spacers are shown in Chart 1. It is envisioned that decoupling of the dansyl label from the copolymer backbone with the longer spacer would allow partitioning into the hydrophobic clusters. Less partitioning would be expected with the short-spaced label since its motion is more directly coupled to that of the backbone. In order to study the pH-induced, globule-to-extended chain response, total polymer concentration was maintained at 0.50 g/L, as shown in Table 1. To accomplish this, labeled polymer was diluted with unlabeled C8 (*n*-octylamide)-modified polymer.

Fluorescence Lifetime. Figure 1 shows the fluorescence emission decay and fitting curves along with the residuals for the long-spaced dansyl labels at pH 2.0 (a) and pH 9.0 (b) analyzed with FLDA. The fitting functions demonstrate double-exponential components for the 30% *n*-octylamide-modified copolymers with both spacers (C8-D2 and C8-D8) for pH values between 5.0 and 6.7. Outside this pH range, single-exponential fits are observed. Single exponentials are also noted over the entire pH range for unmodified C0-D2 and C0-D8 samples.

Figure 2 shows typical fluorescence lifetime distributions for the modified copolymers with long-spaced dansyl labels, C8-D8, at pH values of 2.0, 6.3, and 9.0, respectively. For pH values below 5.0, a broad fluorescence lifetime distribution peak, which has a relatively long mean lifetime value of ~20 ns, is observed. This is consistent with the labels being distributed within a hydrophobic microenvironment. For pH values above 6.7, a narrow fluorescence lifetime distribution peak is

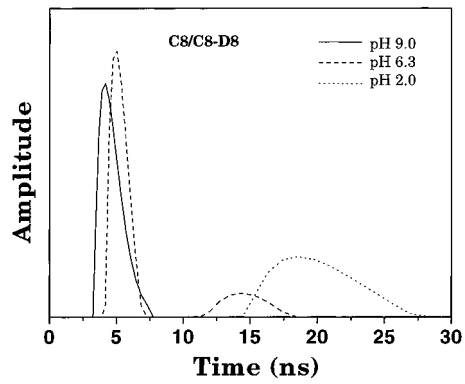

Figure 2. Typical fluorescence lifetime distributions for the C8-modified copolymers with long-spaced dansyl labels at pH values of 9.0, 6.3, and 2.0. λ_{ex} = 330 and λ_{em} = 540 nm.

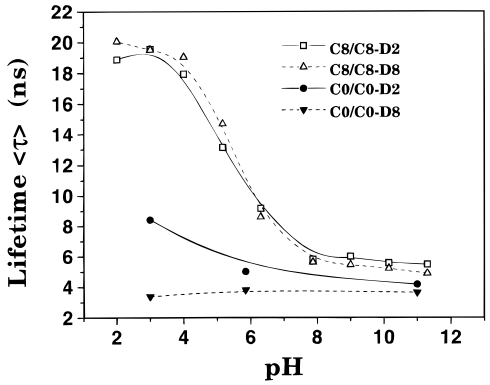

Figure 3. Fluorescence lifetimes analyzed by fluorescence lifetime distribution analysis for C8-modified (C8/C8-D2 and C8/C8-D8) and unmodified copolymers (C0/C0-D2 and C0/C0-D8) as a function of pH.

seen with a relatively short mean lifetime of ~6 ns, indicating that the labels are in direct contact with the aqueous environment. However, between pH values of 5.0 and 6.7, two fluorescence lifetime distributions exist: a narrow fluorescence lifetime distribution with a mean lifetime of ~6 ns and a broad fluorescence lifetime distribution with a mean lifetime of ~14 ns. Clearly, the dansyl labels are distributed between two local environments possessing different characteristics. A narrow lifetime distribution peak of 6 ns is observed for the dansyl labels covalently attached to the unmodified copolymers at all pH values (data not shown), indicating a single hydrophilic microenvironment with no indication of microheterogeneous, associative domains.

Figure 3 shows changes in the mean fluorescence lifetimes of the dansyl labels for the *n*-octyl-modified and unmodified copolymer systems as a function of pH. Since double-exponential components exist for modified copolymers, as determined by FLDA at pH values between 5.0 and 6.7, the average lifetimes of the dansyl labels, $\langle\tau\rangle$, as calculated by eq 5 are shown in Figure 3 and listed in Table 2.

$$\langle\tau\rangle = \sum \tau_i[A_i\%] \qquad i = 2 \tag{5}$$

For pH values above 8.0, the mean fluorescence lifetimes remain constant at ~6.0 ns for both the long- and short-spaced dansyl labels, as shown in Figure 3. However, increases in the fluorescence lifetimes are observed as the pH decreases from 8.0 (~6.0 ns) to 2.0 (~20 ns). The mean fluorescence lifetime values for the unmodified copolymers change little relative to the

Table 2. Fluorescence Decay Parameters[a] of Dansyl Labels between pH 5.0 and 6.7

	long-spaced dansyl				short-spaced dansyl			
pH	τ_1 (ns)	A_1	τ_2 (ns)	A_2	τ_1 (ns)	A_1	τ_2 (ns)	A_2
5.16	16.26	0.849	6.02	0.151	14.68	0.849	4.46	0.151
6.30	15.07	0.359	5.42	0.641	14.06	0.477	4.71	0.523

[a] $I(t) = A_1 \exp(-t/\tau_1) + A_2 \exp(-t/\tau_2)$. See text for explanation of A and τ.

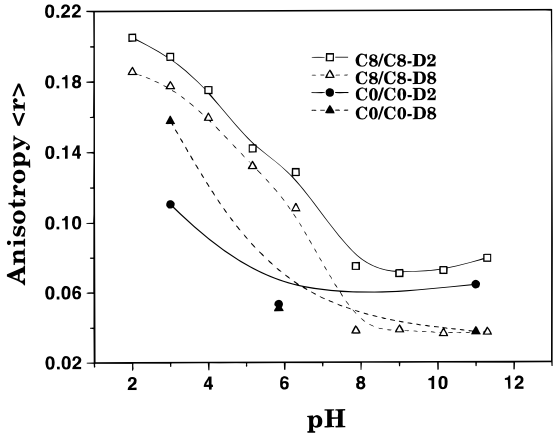

Figure 4. Average steady-state fluorescence anisotropy, $\langle r \rangle$, for the C8-modified and unmodified copolymers having dansyl labels of different spacer lengths as a function of pH. λ_{ex} = 330 and λ_{em} = peak wavelength ±35 nm.

modified copolymers. Only those samples having short-spaced labels (C0-D2) exhibit a slight increase of the fluorescence lifetimes with decreasing pH. Enhanced hydrophobic interactions among the pendently attached *n*-octyl moieties clearly result in intramolecular microheterogeneous domain formation, as evidenced by the much longer fluorescent lifetimes for the labels at low pH as compared to those of the unmodified copolymers in Figure 3.

It may also be noted in Figure 3 that at pH values below 6.7, the mean lifetime values for *n*-octylamide-substituted copolymers with the long-spaced dansyl labels (C8-D8) are shorter than those with short-spaced dansyl labels (C8-D2). In this case, the long-spaced dansyl labels appear to be more strongly associated within the hydrophobic microdomains than the short-spaced labels. However, above pH 6.7, the magnitude of the lifetime values for the long- and short-spaced dansyl labels are reversed. This indicates that the longer spacer length allows more contact with the aqueous media in the absence of hydrophobic microdomains, and the short-spaced dansyl labels experience a more hydrophobic microenvironment due to their proximity to the copolymer backbone.

Fluorescence Anisotropy. SSFA is a measure of the overall mobility of the chromophores. A larger value of the average SSFA, $\langle r \rangle$, indicates a lower mobility for the chromophore being studied, provided the lifetime of the chromophore remains constant. Figure 4 shows $\langle r \rangle$ as a function of pH at 25 °C for dansyl labels bound to hydrophobically modified and unmodified copolymers. For pH values above 6.7, $\langle r \rangle$ is relatively constant for both the long- and short-spaced dansyl labels, but as the pH values decrease from 6.7, $\langle r \rangle$ increases quite dramatically. Across the entire pH range, the $\langle r \rangle$ values for the short-spaced dansyl labels are larger than those for the long-spaced dansyl labels. The same trend is observed for the unmodified copolymers; however, the $\langle r \rangle$ values are substantially less than those of the

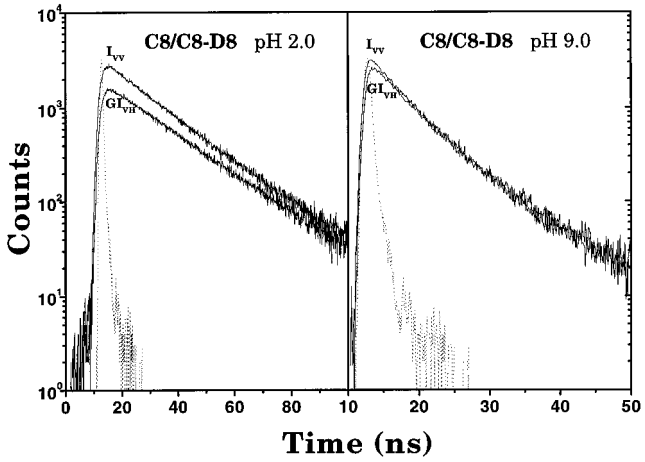

Figure 5. Typical components of the fluorescence anisotropy decays for C8-modified copolymers having long-spaced dansyl labels (C8/C8-D8) at pH values of 2.0 and 9.0. λ_{ex} = 330 nm and λ_{em} = 540 nm.

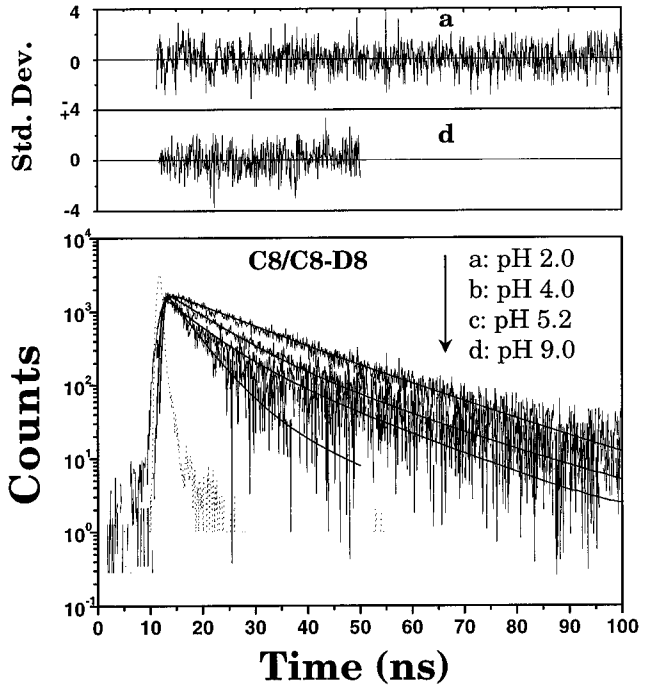

Figure 6. Difference decays, $D(t)$, and their impulse reconvolution fitting curves for the fluorescence anisotropy decays of the C8-modified copolymers having long-spaced dansyl labels at pH values of 2.0, 4.0, 5.2 (fit with a double-exponential function), and 9.0 (fit with a single-exponential function).

modified polymers, indicating that the hydrophobic groups decrease the mobility of the dansyl labels over the entire pH range.

TRFA yields information about the dynamic processes governing the motion of the dansyl labels in different dimensions. Figure 5 shows representative data corresponding to the components of the TRFA decays for the modified copolymer with long-spaced dansyl labels at pH values of 2.0 and 9.0. At pH 2.0, the intensity component analyzed with respect to the parallel plane, $I_{VV}(t)$, is stronger than that analyzed with respect to the perpendicular plane, $GI_{VH}(t)$, for the entire lifetime measurement of 100 ns. At a pH value of 9.0, the parallel component, $I_{VV}(t)$, has the same intensity as the perpendicular component, $GI_{VH}(t)$, after 25 ns.

The difference decay components in TRFA, $D(t)$, their IRA fitting curves, and standard deviations are shown

Table 3. Rotational Correlation Times of Dansyl Labels as a Function of pH As Determined by Impulse Reconvolution Analysis of Time-Resolved Fluorescence Anisotropy

	single exponential[a]					double exponential[b]						
pH	θ_3 (ns)	B_3	r_∞	r_0[c]	χ^2	θ_1 (ns)	B_1	θ_2 (ns)	B_2	r_∞	r_0[c]	χ^2
						C8/C8-D8						
2.00	24.22	0.103	0.110	0.213	1.091	50.98	0.047	9.160	0.056	0.110	0.213	1.094
3.00	23.03	0.160	0.091	0.221	1.138	38.18	0.095	8.798	0.110	0.092	0.227	1.137
4.00	15.28	0.179	0.076	0.235	1.119	30.41	0.101	8.019	0.125	0.074	0.248	1.081
5.16	14.32	0.093	0.039	0.241	1.494	18.28	0.040	8.080	0.060	0.038	0.240	1.501
6.30	3.883	0.057	0.020	0.195	1.300	4.204	0.022	4.091	0.035	0.021	0.196	1.302
7.87	1.275	0.129	0.017	0.193	1.064							
9.00	0.832	0.155	0.015	0.177	1.209							
10.15	0.663	0.190	0.017	0.173	1.159							
11.30	0.879	0.103	0.018	0.155	1.120							
						C8/C8-D2						
2.00	21.71	0.124	0.133	0.258	1.018	32.96	0.100	5.902	0.042	0.122	0.265	1.016
3.00	17.09	0.180	0.079	0.239	1.151	29.69	0.136	6.605	0.044	0.077	0.239	1.154
4.00	16.19	0.160	0.053	0.213	1.122	24.58	0.128	6.319	0.039	0.055	0.216	1.122
5.16	8.182	0.122	0.049	0.210	1.091	18.32	0.091	6.341	0.092	0.047	0.206	1.046
6.30	3.214	0.090	0.043	0.198	1.726	5.942	0.047	5.095	0.035	0.042	0.198	1.405
7.87	1.766	0.151	0.039	0.190	1.047							
9.00	1.339	0.146	0.032	0.178	1.105							
10.15	1.491	0.155	0.041	0.196	1.022							
11.30	1.384	0.170	0.045	0.215	1.208							
						C0/C0-D8						
3.00	2.503	0.157	0.105	0.262	1.049							
5.85	1.321	1.202	0.263	1.465	1.016							
11.00	1.004	1.130	0.186	1.316	1.062							
						C0/C0-D2						
3.00	0.964	1.164	0.367	1.531	0.993							
5.85	0.825	1.232	0.222	1.454	1.055							
11.00	0.790	1.936	0.161	2.097	1.027							

[a] $r(t) = r_\infty + B_3 \exp[t(-t/\theta_3)]$. [b] $r(t) = r_\infty + B_1 \exp[t(-t/\theta_1)] + B_2 \exp[t(-t/\theta_2)]$. [c] $r_0 = r_\infty + \sum B_i$. See text for explanation of θ, B, r_0, r_∞, and χ.

in Figure 6 for C8-D8 copolymers at various pH values. By using IRA, as described in eq 4, the resultant TRFA fitting function is given by

$$r(t) = r_\infty + \sum B_i \exp(-t/\theta_i);\ r_0 = r_\infty + \sum B_i \quad (6)$$

$$i = 1;\ \text{pH} > 6.7 \qquad \text{and} \qquad i = 2;\ \text{pH} < 6.7$$

where r_∞ is the infinite anisotropy, r_0 is the intrinsic anisotropy (the anisotropy at "time zero" following excitation), θ_i is the rotational correlation time, and B_i is the pre-exponential factor that is concerned with the transition angles of the chromophore during the fluorescence emission lifetime. The fitting results from TRFA at various pH values using IRA are listed in Table 3. It should be noted that IRA provides double-exponential resolution up to a pH value of 6.7 for these systems.

The rotational motions of the dansyl labels below a pH value of 6.7 were calculated using a double-exponential function based on a hindered spherelike model.[6,9,15] Using this model, two rotational correlation times, θ_1 and θ_2, are given as

$$(\theta_1)^{-1} = 6D_1 \qquad (\theta_2)^{-1} = 2D_1 + 4D_3 \quad (7)$$

where, D_1 is the rotational diffusion coefficient described by the local motion between the polymer backbone and the chromophore and D_3 is the rotational diffusion coefficient related to the rotational motion of the label about the lever axis. It may be noted that for this model, θ_2 is dominated by D_3 since $D_1 << D_3$ and, therefore, only represents the rotational motion of the chromophore about the lever axis. For pH values above 6.7, a single exponential is sufficient to fit the experimental data, indicating a single process governs the motion of the dansyl labels. Therefore, the hindered spherelike model is simplified to a spherelike model in which the rotational correlation time is given by eq 8, where D_3 is the rotational diffusion coefficient describing the free motion of the chromophore.

$$(\theta_3)^{-1} = 6D_3 \quad (8)$$

Rotational correlation times are shown as a function of pH for both hydrophobically modified and unmodified copolymers having long (Figure 7a,b) and short (Figure 7c,d) spacers to the dansyl labels. The rotational correlation time values in this figure were obtained from SSFA measurements using the Perrin−Weber equation (eq 2) or from TRFA measurements (IRA). The average fluorescence lifetime, $\langle\tau\rangle$, was used to calculate the rotational correlation times from the SSFA, θ, at pH values between 5.0 and 6.7. By comparing the rotational correlation times obtained from SSFA measurements with that from TRFA measurements, one may determine whether the overall mobility of the labels, as measured by the SSFA, θ, is dominated by the motion between the polymer backbone and the chromophore, θ_1, or the rotational motion of the label about the connection lever axis, θ_3.

The values of the rotational correlation times from SSFA decrease smoothly with increasing pH values for all hydrophobically modified copolymers. Values for copolymers with long spacers (C8-D8) correspond more closely with data generated for the single-exponential fitting function (θ_3, Figure 7a) than with data from the double-exponential function (θ_1, Figure 7b). This implies that rotational motion of the labels about the connective lever axis is the primary contributing factor to the SSFA. However, for copolymers with short-spaced labels (C8-D2), rotational correlation times from

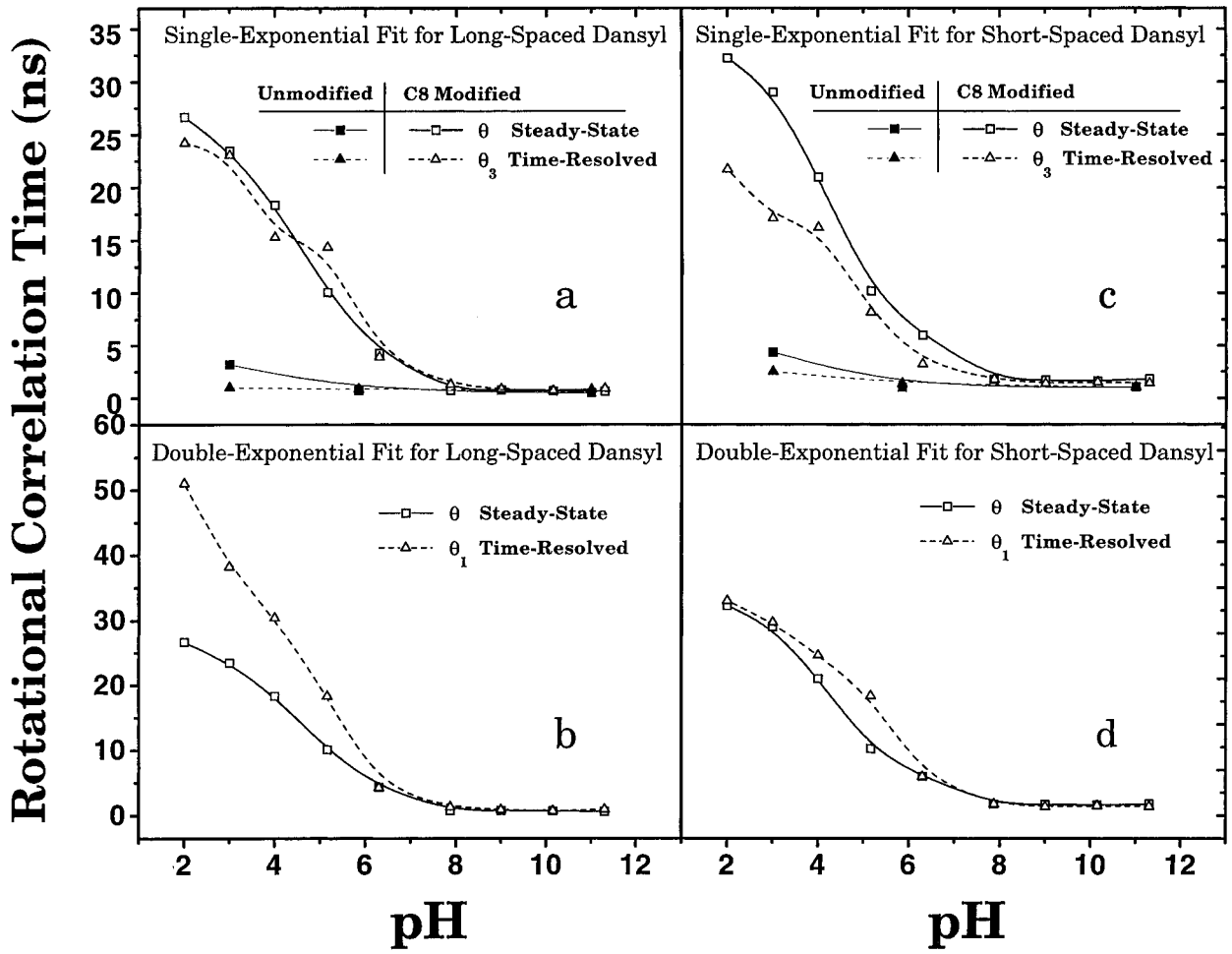

Figure 7. Rotational correlation times from steady-state and time-resolved fluorescence anisotropy measurements as a function of pH for C8-modified and unmodified copolymers with long- (a, b) and short-spaced (c, d) dansyl labels, using single- (a, c) and double-exponential fitting functions (b, d).

the double-exponential fitting function (θ_1, Figure 7d) more closely correspond to the single-exponential fitting function (θ_3, Figure 7c). Therefore, it appears that in this case, the local motion between the dansyl chromophore and the copolymer backbone dominates the SSFA. The fluorescence anisotropy data for the unmodified copolymers having long- and short-spaced labels are also given to illustrate that very little anisotropy is observed in the absence of hydrophobic modification.

In light of the above findings, it may be stated that in the case of the long-spaced dansyl labels, the mobility of the chromophore is restricted to the rotation about the lever axis, θ_3. Therefore, the chromophore is unable to move to a different microenvironment during the fluorescence lifetime and is restricted to the hydrophobic microenvironment at low pH values, as indicated by fluorescence lifetime measurements in Figure 3. Conversely, in the case of the short-spaced dansyl labels, the chromophore is more closely tethered to the polymer backbone and less effectively partitioned into hydrophobic microdomains, as evidenced by the two modes of rotation, θ_1 and θ_2. Therefore, due to the presence of θ_2, the short-spaced dansyl labels are capable of moving from one microenvironment to another during the fluorescence lifetime of the chromophore. This movement of the chromophores between hydrophobic and hydrophilic microenvironments is consistent with the slightly lower fluorescence lifetimes at low pH values, as shown in Figure 3.

By analyzing the local microviscosity around the copolymer backbone and within associative microdomains, it is possible to determine molecular motions and the role they play in the formation of microdomains. Figure 8 shows the rotational diffusion coefficients of the long-spaced (a, b) and short-spaced (c, d) dansyl labels as a function of pH based on the Einstein-type motion of the fluorescent chromophore for a hindered spherelike and a spherelike model, as determined by eq 9.

$$D_1 = \frac{kT}{6\pi\eta a(p+d)^2} \qquad D_3 = \frac{kT}{8\pi\eta a^3} \tag{9}$$

In these equations a is the dansyl label sphere radius, η is the local viscosity, d is the length of the connective lever axis, p is the dynamic persistence length, k is Boltzmann's constant, and T is the absolute temperature.

Parts a and c of Figure 8 show the rotational diffusion coefficient, D_1, which corresponds to the local motion between the polymer backbone and the chromophore. As the pH increases, D_1 also increases with the most dramatic increase occurring near pH = 3.8. This is the pK_{a1} of 3.8 reported for the ionization of the first carboxylic acid group for SM−EVE copolymers.[17,22] This increase in D_1 indicates that the associative hydrophobic microdomains begin to dissipate near the pK_{a1}, and therefore, the motion between the chromophore and copolymer backbone increases dramatically. Parts a

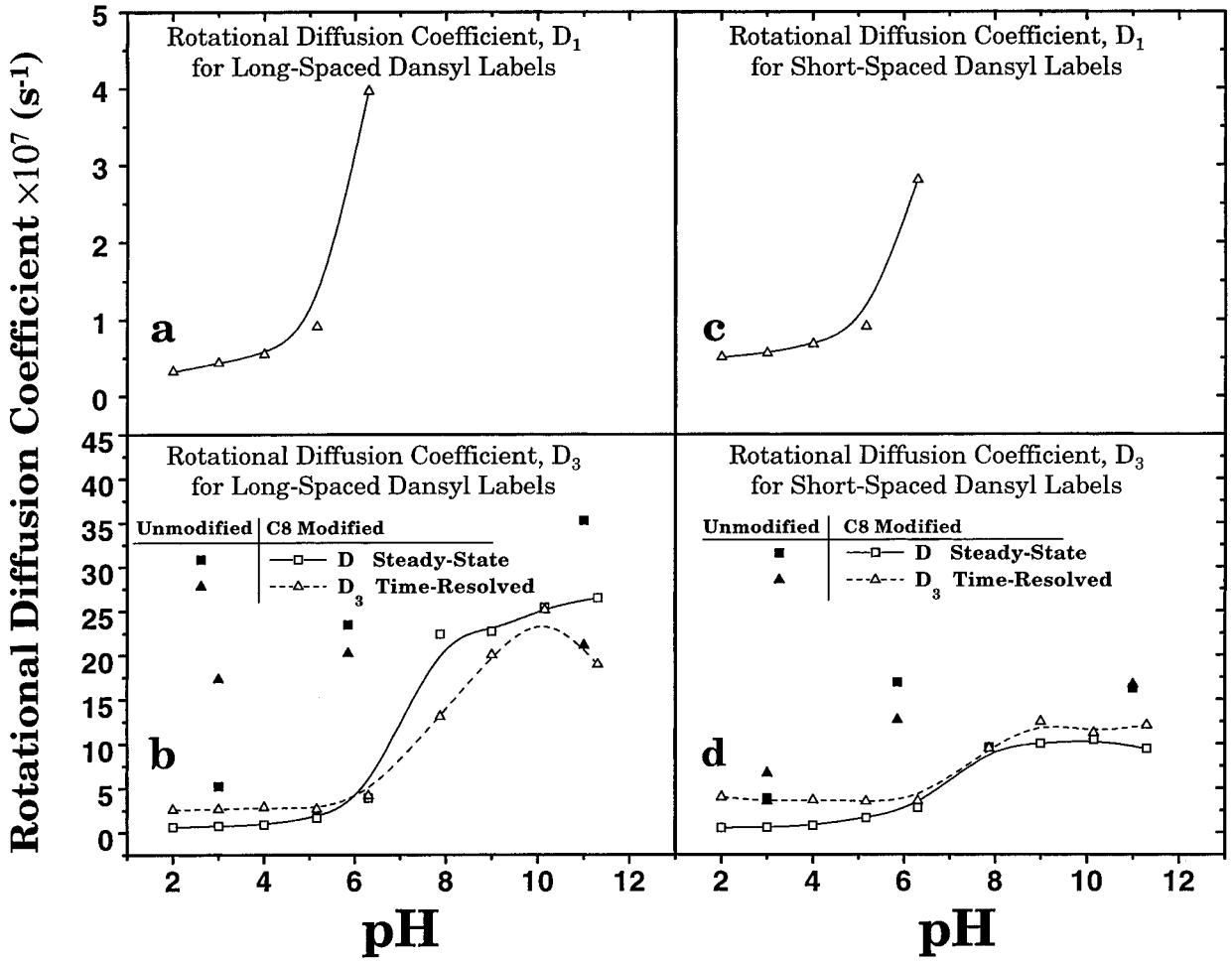

Figure 8. Rotational diffusion coefficients from steady-state and time-resolved fluorescence anisotropy as a function of pH for C8-modified and unmodified copolymers having long- (a, b) and short-spaced (c, d) dansyl labels.

and b of Figure 8 show the rotational diffusion coefficient, D_3, which corresponds to the rotational motion of the labels about the lever axis. As with D_1, the D_3 values increase with increasing pH with the most dramatic increase occurring near $pK_{a2} = 6.6$ corresponding to the ionization of the second carboxylic acid group.[17,22] This indicates that the interior of the hydrophobic aggregate microdomains starts to disassociate near the pK_{a2}, as evidenced by the enhanced rotation of the dansyl chromophore.

Figure 9 shows a change in the relative microviscosity surrounding the long- and short-spaced dansyl labels as a function of pH, as determined using eq 10. In this analysis, it is assumed that the size of the dansyl chromophore at a given pH value is the same despite the length of the spacer.

$$\frac{D_{3\ \mathrm{short}}}{D_{3\ \mathrm{long}}} = \frac{\eta_{\mathrm{short}}}{\eta_{\mathrm{long}}} \tag{10}$$

The viscosity of the microenvironment around the long- and short-spaced dansyl labels, which is related to the rotational friction constant, f, is determined by the complex steric, ionic, and hydrogen-bonding interactions of the solvated labels.[6] In Figure 9, $\eta_{\mathrm{long}}/\eta_{\mathrm{short}}$ decreases with increasing pH values. Below pH 6.7, $\eta_{\mathrm{long}}/\eta_{\mathrm{short}}$ is greater than 1.0, and above pH 6.7, this value is less than 1.0, with the minimum value occurring at pH 10.0. Below pH 6.7, the long-spaced dansyl labels are within the interior of the hydrophobic microdomains. Water has been excluded due to strong

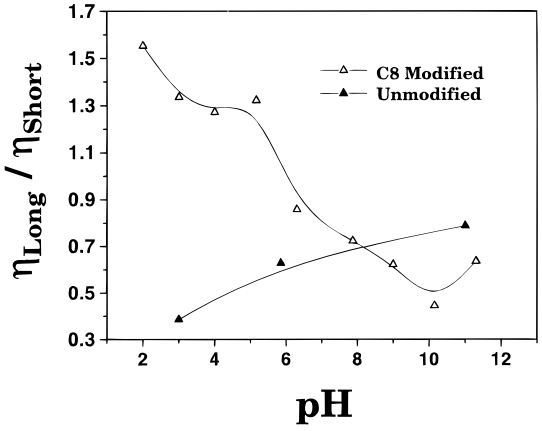

Figure 9. Microviscosity ratio around the long- and short-spaced dansyl labels as a function of pH using impulse reconvolution analyses of time-resolved fluorescence anisotropy for C8-modified and unmodified copolymers.

intramolecular hydrogen bonding. Thus, the rotational motion is hindered as a result of the large rotational friction constant, f. In contrast, the rotational motion of the short-spaced dansyl labels is greater than for the long-spaced labels because the short-spacer length inhibits the partitioning into the hydrophobic associations. At pH values above 6.7, although the motions of the long- and short-spaced dansyl labels are increased due to the extended conformation of the copolymer coil, the microviscosity experienced by the short-spaced dansyl labels is larger than that of the long-spaced

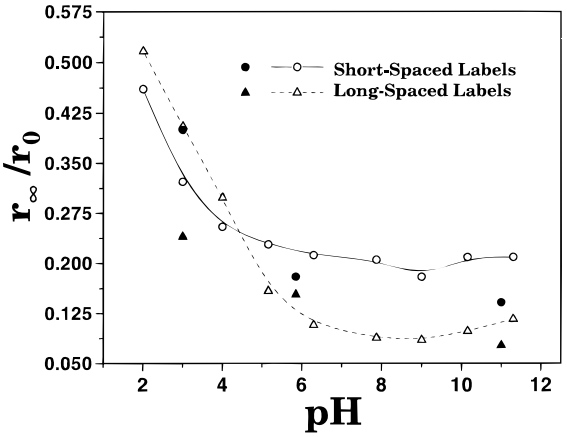

Figure 10. Relative fluorescence values of infinite to intrinsic fluorescence anisotropy, r_∞/r_0, as a function of pH for C8-modified (open symbols) and unmodified (solid symbols) copolymers having dansyl labels with different spacer lengths using impulse reconvolution analysis of time-resolved fluorescence anisotropy.

dansyl labels due to interactions in the vicinity of the copolymer backbone. This is also evidenced by the slightly longer fluorescence lifetimes exhibited by the short-spaced dansyl labels above pH 6.7, as mentioned previously.

Figure 10 shows the ratio of the infinite-to-intrinsic fluorescence anisotropies, r_∞/r_0, for the long- and short-spaced dansyl labels. This ratio expresses the fraction of rotational motion processes of the chromophore having a relaxation time significantly longer than that of the fluorescence lifetime of the labels; i.e. an increase in this ratio indicates that the motion of the fluorescent labels is more hindered. Below a pH value near the pK_{a1}, the ratio, r_∞/r_0, for the long-spaced labels is greater than that for the short-spaced labels due to the more hindered motion of the long-spaced labels. However, above pH values near pK_{a1}, the motion of the short-spaced dansyl labels are more hindered, as mentioned previously. The r_∞/r_0 data for the unmodified polymer exhibit behavior similar to that of the modified copolymers except that the values of r_∞/r_0 are much lower for the unmodified system. Clearly, the chromophores in this case experience more rotational freedom due to the lack of hydrophobic associations.

A simplistic representation of the pH-triggered conformational behavior of 30% *n*-octylamide-modified copoly(SM−EVEs) in dilute aqueous solution consistent with rotational motions of the dansyl labels studied in this work is illustrated in Chart 2. At low pH values, the dansyl labels with long-spacer lengths may more easily partition into hydrophobic microdomains formed by *n*-octyl groups, thus limiting their mobility. The short-spaced labels, being close to the polymer backbone, cannot fully localize within the hydrophobic domains and, therefore, have more freedom for rotational motion at low pH. This is supported by the following evidence: (1) the long-spaced dansyl labels exhibit a longer fluorescence lifetime than the short-spaced labels (Figure 3); (2) the rotational motion of the long-spaced dansyl label about the lever axis is the primary component to the steady-state anisotropy (Figure 7); (3) the long-spaced dansyl labels experience a higher relative microviscosity ($\eta_{long}/\eta_{short} > 1$) (Figure 9); and (4) the long-spaced dansyl labels exhibit higher ratios of r_∞/r_0 below pK_{a1} (Figure 10).

At high pH values, the rotational motion for both the long- and short-spaced labels increases as the polymer

Chart 2. Mechanism of pH-Triggered Association Behavior of 30% *n*-Octylamide-Modified Copoly(SM−EVEs) and Rotational Motion for Dansyl Labels with Different Spacer Lengths

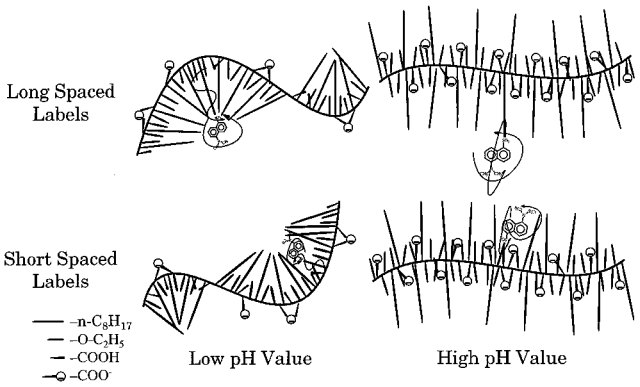

coil expands. However, the extent of increase for the long-spaced labels is greater than that for the short-spaced labels due to the decoupling of the chromophore from the copolymer backbone. The motion of the short-spaced dansyl labels is hindered due to interactions between the chromophore and macromolecular backbone, as supported by the following evidence: (1) the short-spaced dansyl labels exhibit a longer fluorescence lifetime than the long-spaced labels (Figure 3); (2) the short-spaced dansyl labels experience a higher relative microviscosity ($\eta_{long}/\eta_{short} < 1$) (Figure 9); and (3) the short-spaced dansyl labels exhibit higher ratios of r_∞/r_0 than the long-spaced dansyl labels (Figure 10).

Conclusions

The pH-triggered conformational change of unmodified and 30 mol % *n*-octyl hydrophobically modified copoly(sodium maleate-*alt*-ethyl vinyl ethers) in aqueous media has been monitored using transient fluorescence and fluorescence anisotropy techniques. Fluorescent labels having two different spacer lengths were covalently bound to the copolymer backbone in order to monitor molecular motions coupled closely to the copolymer backbone and within associating hydrophobic microdomains.

At pH values below pK_{a1}, the hydrophobically-modified copolymer associates into microheterogeneous domains composed of compact globules as a result of the hydrophobic interactions of the pendently attached *n*-octyl hydrophobes, as evidenced by fluorescence lifetimes and anisotropy behavior. At these low pH values, two rotational motions are observed using time-resolved fluorescence anisotropy measurements: the local motion between the chromophore and copolymer backbone and the rotational motion of the label about the connective lever axis. As the pH increases above pK_{a1}, the microheterogeneous domains begin to dissipate, indicated by the appearance of two distinct fluorescence lifetime distributions and a sharp increase in the motion between the chromophore and copolymer backbone, D_1. At pH values above pK_{a2}, the microheterogeneous domains are completely dissipated when the copolymer assumes an expanded conformation as a result of charge−charge repulsion between the ionized carboxylate moieties. This is indicated by a single, short fluorescence lifetime distribution and a single molecular rotational motion exhibited by the chromophore. This expanded conformation allows the long-spaced dansyl labels to have more rotational freedom than the short-spaced labels, which are closer to the copolymer backbone.

Acknowledgment. Funding from the U.S. Office of Naval Research, the U.S. Department of Energy, and the Gillette Research Institute is gratefully acknowledged.

References and Notes

(1) Bednar, B.; Trnena, J.; Svoboda, P.; Vajda, S.; Fidler, V.; Prochazka, K. *Macromolecules* **1991**, *24*, 2054.
(2) Soutar, I.; Swanson, L.; Imhof, R. E.; Rumbles, G. *Macromolecules* **1992**, *25*, 4399.
(3) Soutar, I.; Swanson, L. *Macromolecules* **1994**, *27*, 4304.
(4) Swaminathan, R.; Periasamy, N.; Udgaonkar, J. B.; Krishnamoorthy, G. *J. Phys. Chem.* **1994**, *98*, 9270.
(5) Fukumura, H.; Hayashi, K. *J. Colloid Interface Sci*, **1990**, *135*, 435.
(6) Ricka, J.; Gysel, H.; Schneider, J.; Nyffenegger, R.; Binkert, T. *Macromolecules* **1987**, *20*, 1407.
(7) Pascal, P.; Duhamei, J.; Wang, Y.; Winnik, M. A.; Zhu, X.; Macdonald, P.; Napper, D. H.; Gilbert, R.; *Polymer* **1993**, *34*, 1134.
(8) Binkert, Th.; Oberreich, J.; Meewes, M.; Nyffenegger, R.; Ricka, J. *Macromolecules* **1991**, *24*, 5086.
(9) Watanabe, A.; Matsuda, M. *Macromolecules* **1986**, *19*, 2253.
(10) Chan, J.; Fox, S.; Kiserow, D.; Ramireddy, C.; Munk, P.; Webber, S. E. *Macromolecules* **1993**, *26*, 7016.
(11) Hu, Y.; Horie, K.; Ushiki, H. *Macromolecules* **1992**, *25*, 6046.
(12) Seo, T.; Take, S.; Akimoto, T.; Hamada, K.; Iijima, T. *Macromolecules* **1991**, *24*, 4801.
(13) Bednar, B.; Morawetz, H.; Shafer, J. A. *Macromolecules* **1985**, *18*, 1940.
(14) Li, Y. H.; Chan, L. M.; Tyer, L.; Moody, R. T.; Himel, C. M.; Hercules, D. M. *J. Am.Chem.Soc.* **1975**, *97*, 3118.
(15) Hu, Y.; Horie, K.; Ushiki, H. *Polym. J.* **1993**, *25*, 651.
(16) Hu, Y.; Smith, G. L.; Richardson, M. F.; McCormick, C. L. *Macromolecules* **1997**, *30*, 3526.
(17) Strauss, U. P.; Gershfeld, N. L. *J. Phys. Chem.* **1954**, *48*, 747.
(18) O'Connor, D. V.; Philips, D. *Time-Correlated Single Photon Counting*; Academic Press: New York, 1984.
(19) Webber, G. *Biochem. J.* **1952**, *51*, 145, 155.
(20) Barkly, M. D.; Kowalczyk, A. A. Grand, L. *J. Chem. Phys.* **1981**, *75*, 3581.
(21) Wahl, P. *Chem. Phys.* **1975**, *7*, 210.
(22) Strauss, U.; Vesnaver, G. *J. Phys. Chem.* **1975**, *79*, 1558, 2426.

MA9617532